Supporting Information

1. Experimental Section

1.1 Materials Fabrication and measurement of devices

PBDB-T, PM6 and PM7 were purchased from Solarmer Materials Inc. PYT were synthesized in our lab as reported previously.[1, 2] The aqueous dispersion of PEDOT:PSS was purchased from Heraeus, Germany. Chloroform was dried and distilled from appropriate drying agents prior to use.

1.2 Fabrication and measurement of devices

Solar cells were fabricated in the configuration of the traditional sandwich structure with an indium tin oxide (ITO) glass positive electrode and a poly[9,9-bis[6(N,N,Ntrimethylammonium)hexyl]fluorene-alt-co-1,4-phenylene]-bromide (PFN-Br) / silver (Ag) negative electrode. The ITO-based substrates were pre-cleaned in an ultrasonic bath of detergent, deionized water, acetone and isopropanol, and an UV-treated in ultraviolet-ozone chamber (Jelight Company, USA) for 15 min. A thin layer of PEDOT:PSS (poly(3,4-ethylene dioxythiophene): poly(styrene sulfonate)) was spin-coating at 4000 rpm for 30s on the ITO substrate. And then, PEDOT:PSS film was baked at 150 ºC for 15 min in the air, and thickness is approximately ~40 nm. PBDB-T:PYT all-polymer blend solutions (16 mg/mL, D/A ratio=1/1.2) in blend solution (CF/CN=97/3, vol%) were kept stirring for at least 12h.[3] PM6 (PM7):PYT all-polymer blend solutions (16 mg/mL, D/A ratio=1/1.2) in blend solution (CF/CN=99/0.5, vol%) were kept stirring for at least 12h.[2] All-polymer active layer was spin-coated onto the top of PEDOT:PSS layer at varying spin-coating rates for 30s, which was further thermally annealed at 110℃ for 10 min in the glovebox. The thicknesses of the active layers are about 100 nm. The thickness of the active layer is measured by a surface

profiler (Alpha-Step 500, KLA-Tencor, USA). For all types of devices, a methanol solution of PFN-Br at a concentration of 0.5 mg mL^{-1} was spin-coated onto the photoactive layer at 3000 r.p.m. for 30 s. Finally, top Ag (Hebei Qinbang New Material Technology Co., Ltd) electrode of 100 nm thickness was evaporated in vacuum onto the cathode buffer layer at a pressure of 5×10^{-6} mbar. In our work, the typical active area of the investigated devices was 5 mm^2.

The current-voltage characteristics of the solar cells were measured under AM 1.5 G irradiation on an Enli Solar simulator (100 mW cm^{-2}). Before each test, the solar simulator was calibrated with a standard single-crystal Si solar cell (made by Enli Technology Co., Ltd., Taiwan, calibrated by The National Institute of Metrology (NIM) of China). Short circuit currents under AM1.5 G (100 $mWcm^{-2}$) conditions were estimated from the spectral response and convolution with the solar spectrum. The external quantum efficiency was measured by a Solar Cell Spectral Response Measurement System QE-R3011 (Enli Technology Co., Ltd.). A calibrated silicon detector was used to determine the absolute photosensitivity at different wavelengths.

1.3 Morphology measurements

Atomic Force Microscopy (AFM) images were obtained by using Nano Wizard 4 atomic force microscopy (JPK Inc. Germany) in QI mode to observe the surface morphologies of the different films deposited on glass substrates. For the probe, we select the Triangular pyramid probe (BRUKER, NCHV-A model). During the process of observation, scan speed is 58.2 μm/s and the size is 5 × 5 μm^2.

GIWAXS/GISAXS measurements with Kα X-ray of Cu source (8.05 keV, 1.54 Å) and a Pilatus3R 300 K detector were conducted at a Xeuss 2.0 SAXS/WAXS laboratory beamline. Samples were prepared by spin coating identical chloroform blend solutions as those used in PSCs on Si substrates. The grazing incident angle was 0.2°.

1.4 Physical tests

Transient photovoltage (TPV) measurements: For TPV measurements, devices were directly connected to an oscilloscope in open-circuit conditions (1MΩ). Then the device was illuminated with a white light LED at different light intensities. A small optical perturbation was applied using a 405 nm laser-diode which was adjusted in light intensity to produce a voltage perturbation of $\Delta Vo < 10\,mV \ll Voc$. The amount of charges generated by the pulse was obtained by integrating a photocurrent measurement (50 Ω) without bias light.

Charge extraction (CE) measurements: For CE measurements, it can be used to determine the charge density in the active layer of the device at any point in the *J-V* curve. The devices were held at a specified voltage in the dark or under illumination. At a certain time t_0 the light is switched off, the cell is switched to short-circuit conditions, and the resulting current transient is recorded with an oscilloscope. Most of the charge is extracted in a few microseconds due to a high internal electrical field at short circuit conditions. In addition, a fast analog switch from Texas Instruments (TS5A23159) is used to perform the switching from the specified voltage to short circuit conditions. It provides a very quick switching time (50 ns), a low on-state resistance (1 Ω), high off-state resistance (> 1MΩ) and a very low charge injection (<< 10^{15} $cm^2V^{-1}s^{-1}$). A Keithley 2440 source-measurement unit is used to set the initial device voltage.

Transient absorption spectroscopy (TAS): For femtosecond transient absorption spectroscopy, the fundamental output from Yb: KGW laser (1030 nm, 220 fs Gaussian fit, 100 kHz, Light Conversion Ltd) was separated into two light beams. One was introduced to NOPA (ORPHEUS-N, Light Conversion Ltd) to produce a certain wavelength for pump beam (750 nm, below 10 $\mu J/cm^2$/pulse, 30 fs pulse duration), the other was focused onto a YAG plate to generate white light continuum as the probe beam. The pump and probe overlapped on the sample at a small angle of less than 10°. The transmitted probe light from the sample was collected by a linear CCD array. All the samples were tested in vacuum.

1.5 Space charge limited current (SCLC) measurements

Single carrier devices were fabricated, and the dark current-voltage characteristics were measured and analyzed in the space charge limited current (SCLC) regime following the references. The structure of hole-only devices was Glass/ITO/PEDOT:PSS/active layer/MoO_3 (10 nm)/Ag (100 nm). For the electron-only devices, the structure was Glass/ITO/ZnO/active layer/PFN-Br/Ag (100 nm), where Ag was evaporated. Mobilities were extracted by fitting the current density-voltage curves using the Mott-Gurney relationship. The reported mobility data are average values over the six devices of each sample.

1.6 Stability measurements

We performed the long-time thermal and light experiments of the unencapsulated all-polymer devices investigated in this study, measured under 85 ℃ hotplate and light stability under one sun illumination at room temperature in an N_2-filled glovebox for 408 hours. In detail, the long-term stability of unencapsulated devices was conducted with a glove-box integrated multichannel solar cell performance decay test system fabricated by our group under a testing condition in accordance with ISOS-L-1. The devices were put inside a nitrogen-filled glovebox (H_2O < 1 ppm, O_2 < 1 ppm) and continuously illuminated with a white LED array (XLamp CXA1512 6500K CCT). The illumination light intensity was initially set before testing to make sure the output short-circuit current density equals the value that was measured under standard conditions mentioned earlier, and it was monitored by a photodiode (Hamamtsu S1336-8BQ) to guarantee stable light intensity. *J-V* characters of the devices were checked periodically, and the photovoltaic parameters were calculated automatically according to the achieved *J-V* curves. Notably, the photovoltaic parameters of devices under illumination were recorded over time automatically and the degradation curves were shown. The cell temperature was measured occasionally, and the temperature range during aging was approximately 30 ^oC. The solar cells were fabricated in a glovebox and aged in the same conditions, excluding the well-known effects of oxygen and water

degradation from our experiments.

2. Tables and Figures

Table S1. Molecular weight and optoelectronic properties of the investigated polymers.

Sample	M_w (kg/mol)	PDI	λ_{max} (nm)[b]	λ_{edge} (nm)	HOMO (eV)[c]	LUMO (eV)[c]
PBDB-T	97.6	1.87	623	676	5.34	3.32
PM6	97.7	2.15	612	681	5.47	3.61
PM7	93.3	2.37	611	681	5.52	3.57
PYT-M[a]	20.5	1.67	815	932	5.69	3.92
PYT-H[a]	38.3	1.86	815	932	5.69	3.93

[a] The data of molecular weight are determined by GPC, which comes from our previous paper[4, 5].

[b] absorption spectra of relevant neat films. [c] the data come from the previous paper[4, 5].

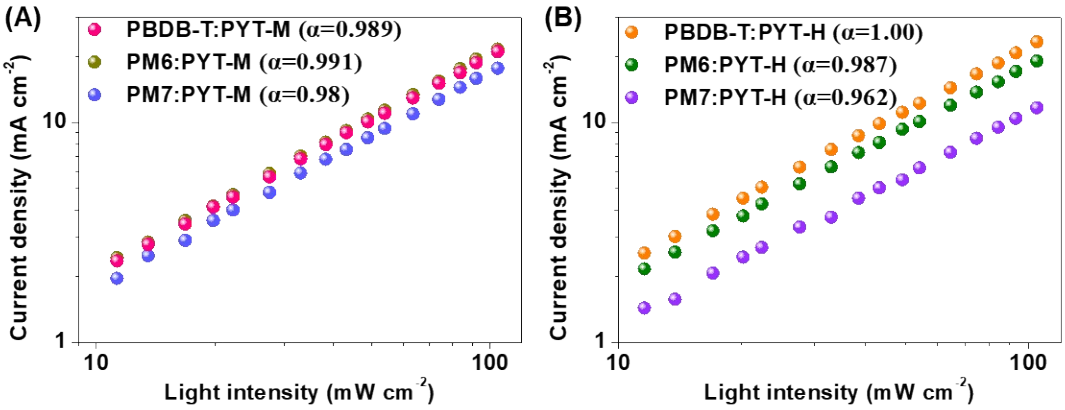

Figure S1. Measurement of J_{SC} *versus* light intensity for (A) the -PYT-M-based all-polymer devices and (B) the PYT-H-based all-polymer devices, respectively.

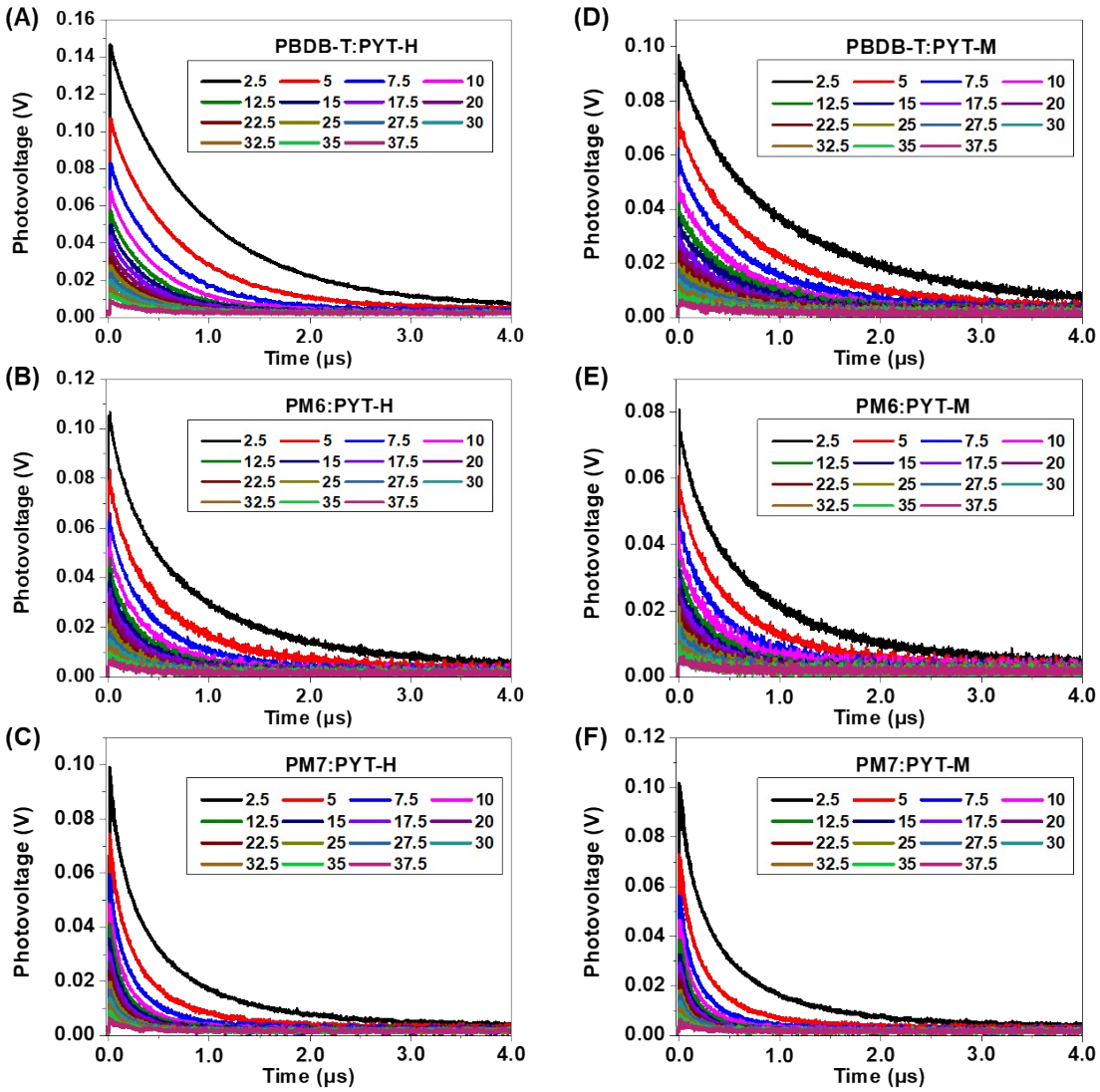

Figure S2. TPV measurements on the PBDB-T(PM6, PM7):PYT-H (A-C) and PBDB-T(PM6, PM7):PYT-M (D-F) devices for light intensities of 0.15 to 2.50 sun. Transient photovoltage (TPV) measurements were used to analyze the recombination of free charges within the working devices by recording the transient voltage decay of the device under open-circuit conditions under continuous illumination before a small perturbative light pulse was injected.

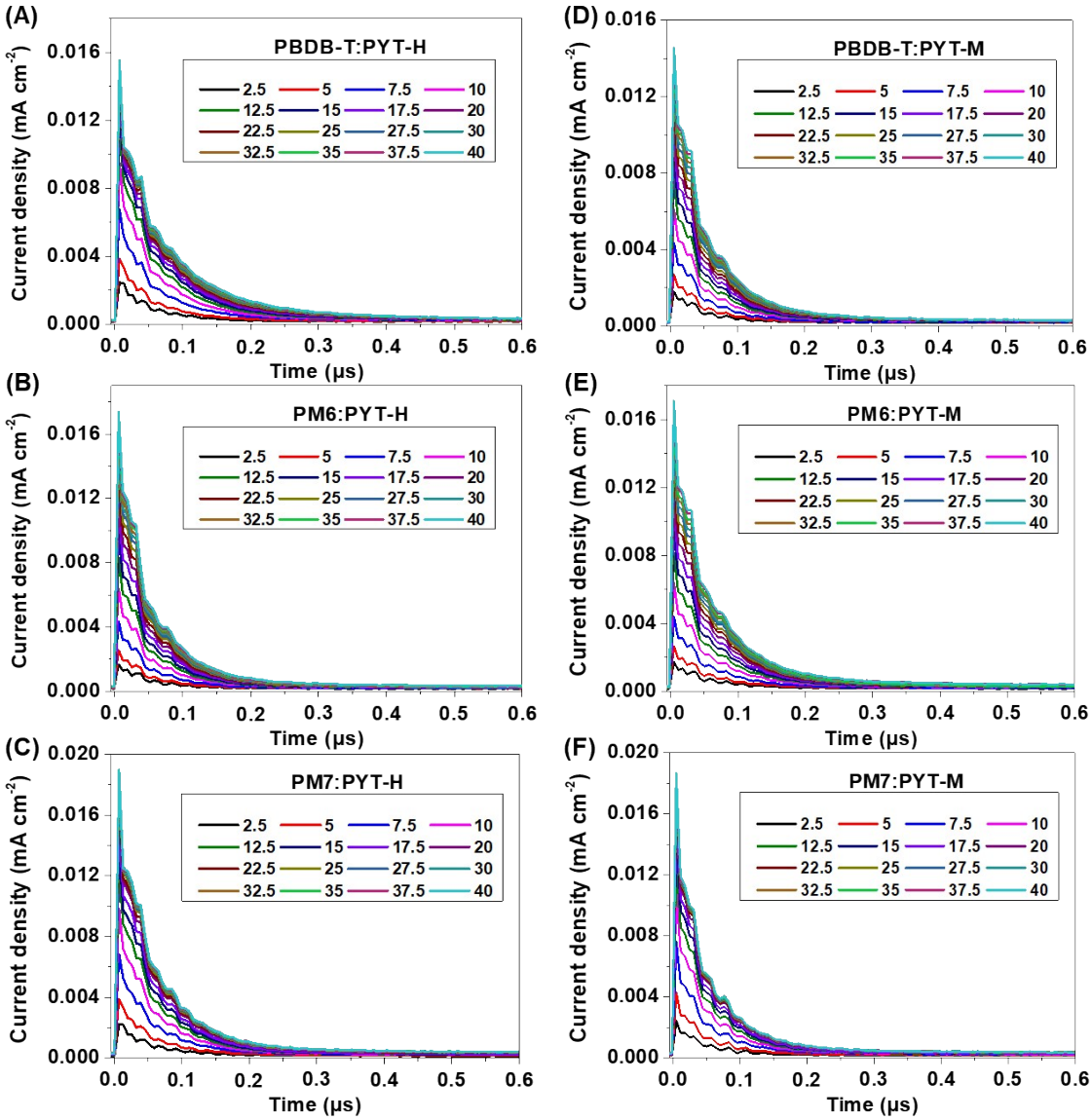

Figure S3. CE measurements on the PBDB-T(PM6, PM7):PYT-H (A-C) and PBDB-T(PM6, PM7):PYT-M (D-F) devices for light intensities of 0.15 to 2.50 sun.

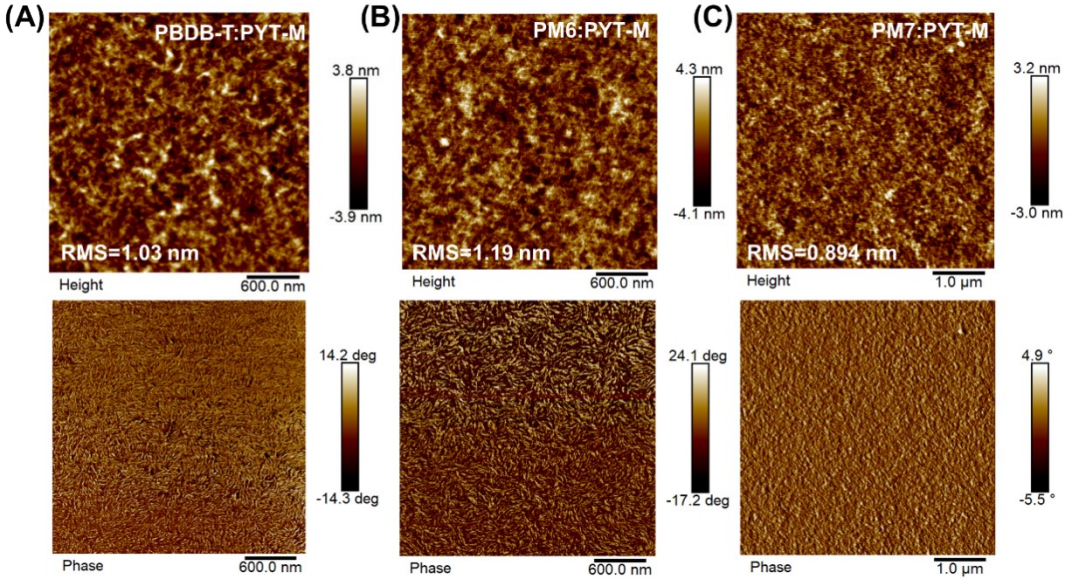

Figure S4. Contact mode AFM surface scans of blend films of (A) PBDB-T:PYT-M (RMS roughness:1.03 nm), (B) PM6:PYT-M (RMS roughness:1.19 nm), (C) PM7:PYT-M (RMS roughness:0.89 nm).

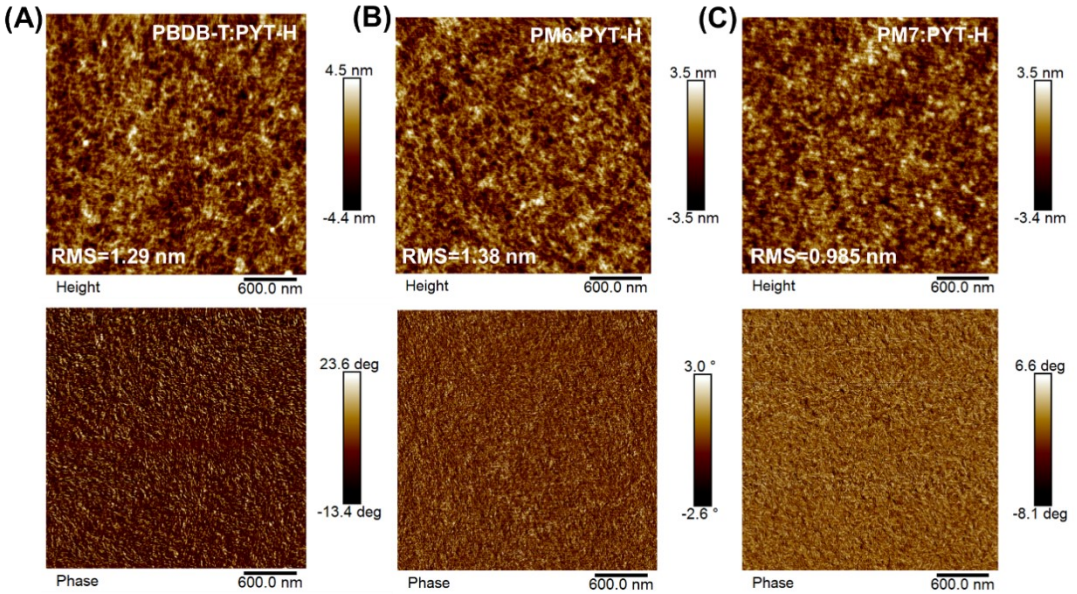

Figure S5. Contact mode AFM surface scans of blend films of (A) PBDB-T:PYT-H (RMS roughness:1.29 nm), (B) PM6:PYT-H (RMS roughness:1.38 nm), (C) PM7:PYT-H (RMS roughness:0.99 nm).

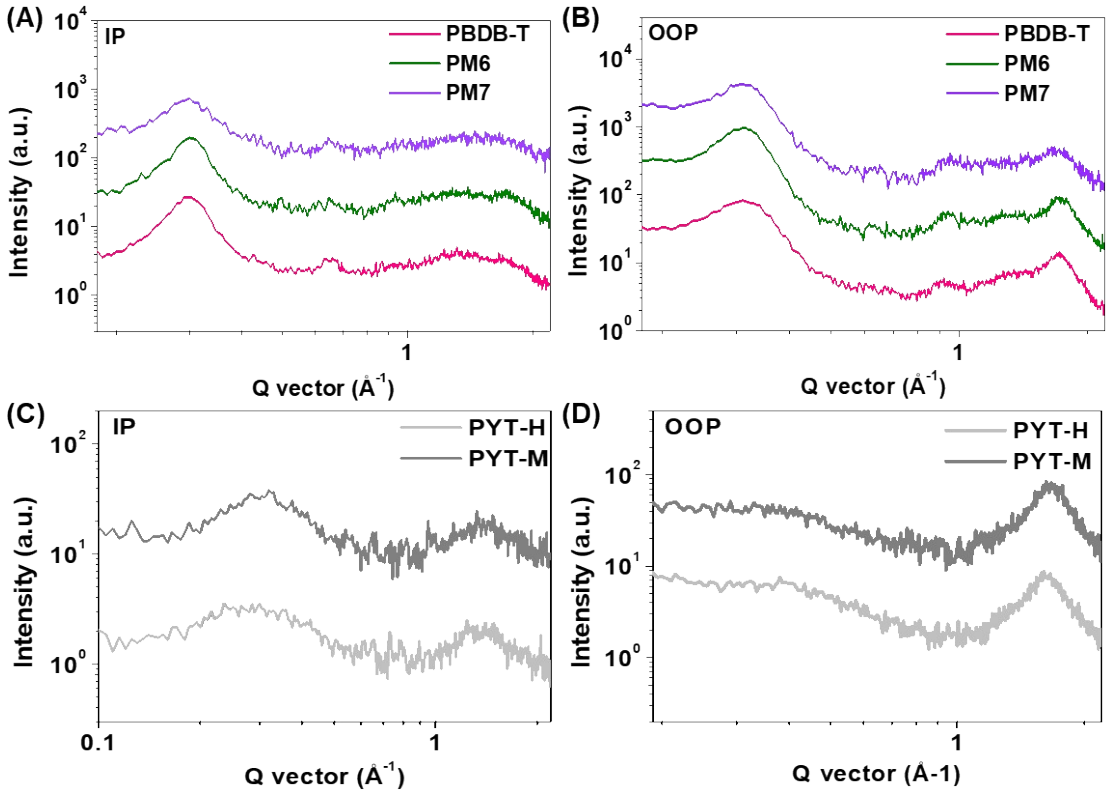

Figure S6. Scattering profiles of in-plane (IP) and out-of-plane (OOP) for (A-B) the PBDB-T, PM6 and PM7 neat films and (C-D) the PYT (PYT-H and PYT-M) neat films.

Table S2. Summary of the extracted data from the GIWAXS patterns of the pristine PBDB-T and PYT films.

Sample	IP (100)		OOP (010)	
	Q value (Å^{-1})	Lattice spacing (Å)	FWHM (Å^{-1})	Coherence length (Å)
PBDB-T	0.297	21.16	0.21	29.92
PM6	0.297	21.16	0.23	27.32
PM7	0.297	21.16	0.44	14.28
PYT-M	0.32	19.63	0.335	18.76
PYT-H	0.31	20.27	0.323	19.45

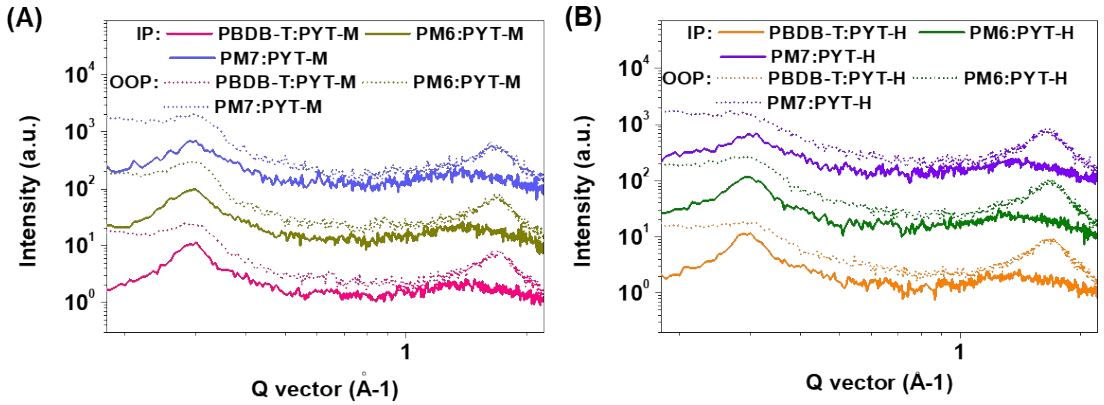

Figure S7. Scattering profiles of in-plane (IP) and out-of-plane (OOP) for (A) the PBDB-T (PM6, PM7):PYT-M blends and (B) PBDB-T (PM6, PM7):PYT-H films.

Table S3. Summary of the extracted data from the GIWAXS patterns of the different blends films.

Donor:Acceptor		IP (100)		OOP (010)	
		Q value ($Å^{-1}$)	Lattice spacing (Å)	FWHM ($Å^{-1}$)	Coherence length (Å)
PYT-M	PBDB-T	0.30	20.94	0.336	18.70
	PM6	0.30	20.94	0.330	19.03
	PM7	0.30	20.94	0.343	18.31
PYT-H	PBDB-T	0.298	21.08	0.325	19.33
	PM6	0.299	21.01	0.307	20.47
	PM7	0.309	20.33	0.330	19.04

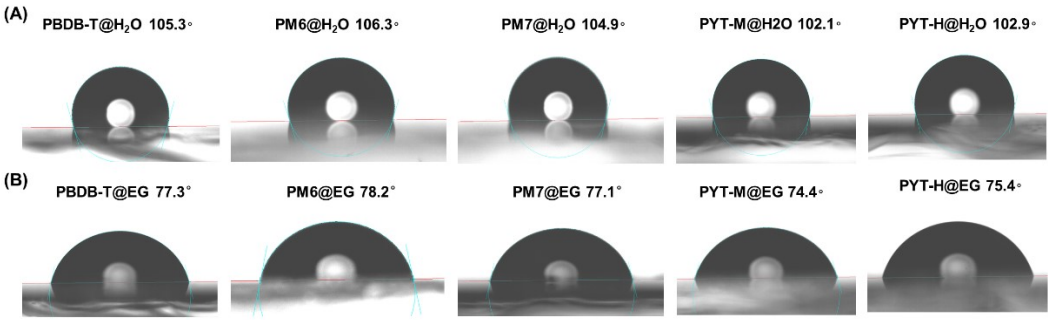

Figure S8. Photographs of water (A) and ethylene glycol (EG, B) droplets on the top surfaces of the neat PBDB-T, PM6, PM7, PYT-M and PYT-H films, and the respective contact angle values. The contact angle measurement is conducted at the center of the substrates, avoiding the edges, reflecting the properties of the effective working area in the devices.

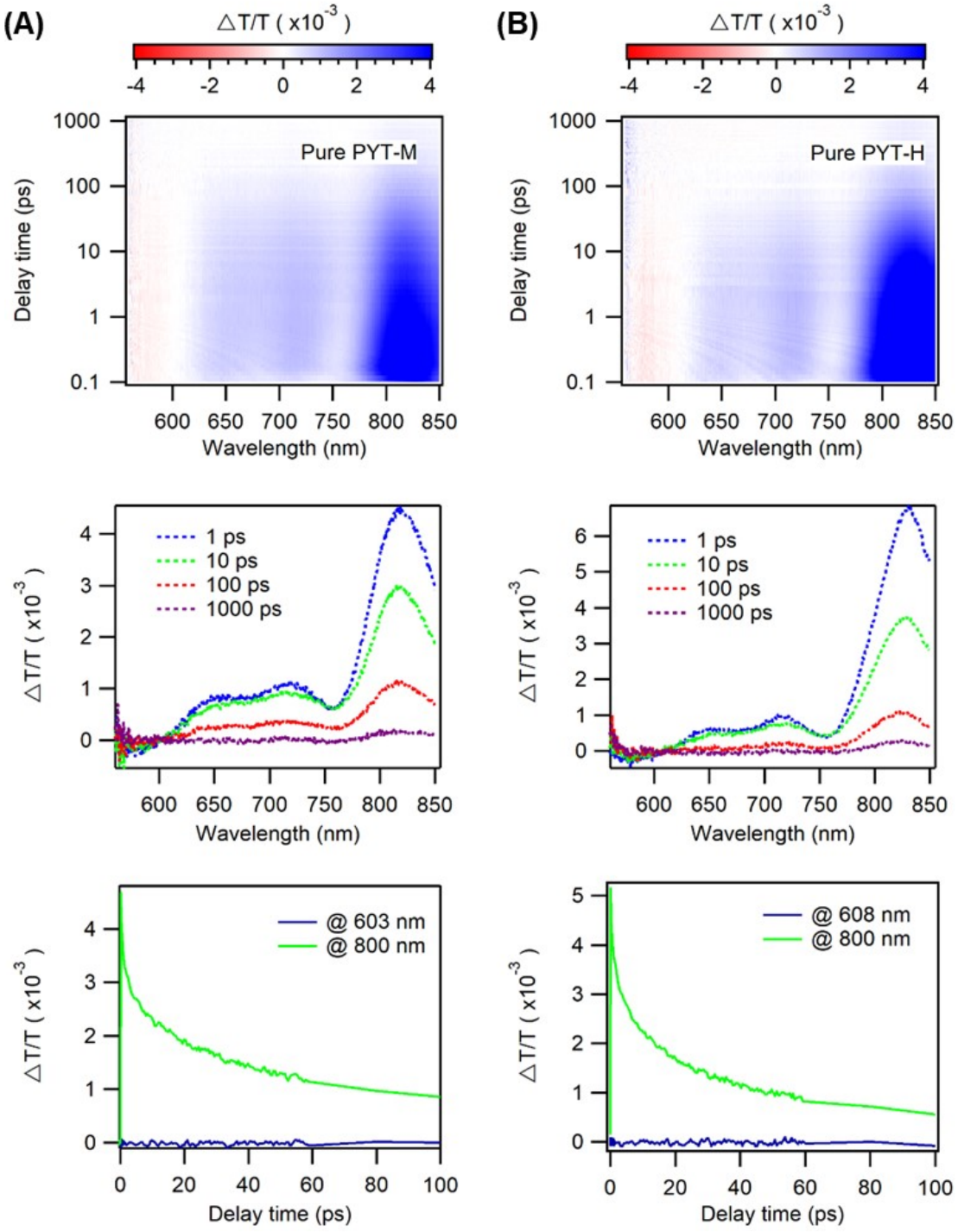

Figure S9. Femtosecond TA dynamics for the different films. 2D color plot of transient absorption spectra of the (A) pristine PYT-M and (B) PYT-H films. As well as transient absorption spectra of the pristine PYT-M and PYT-H films at indicated delay times.

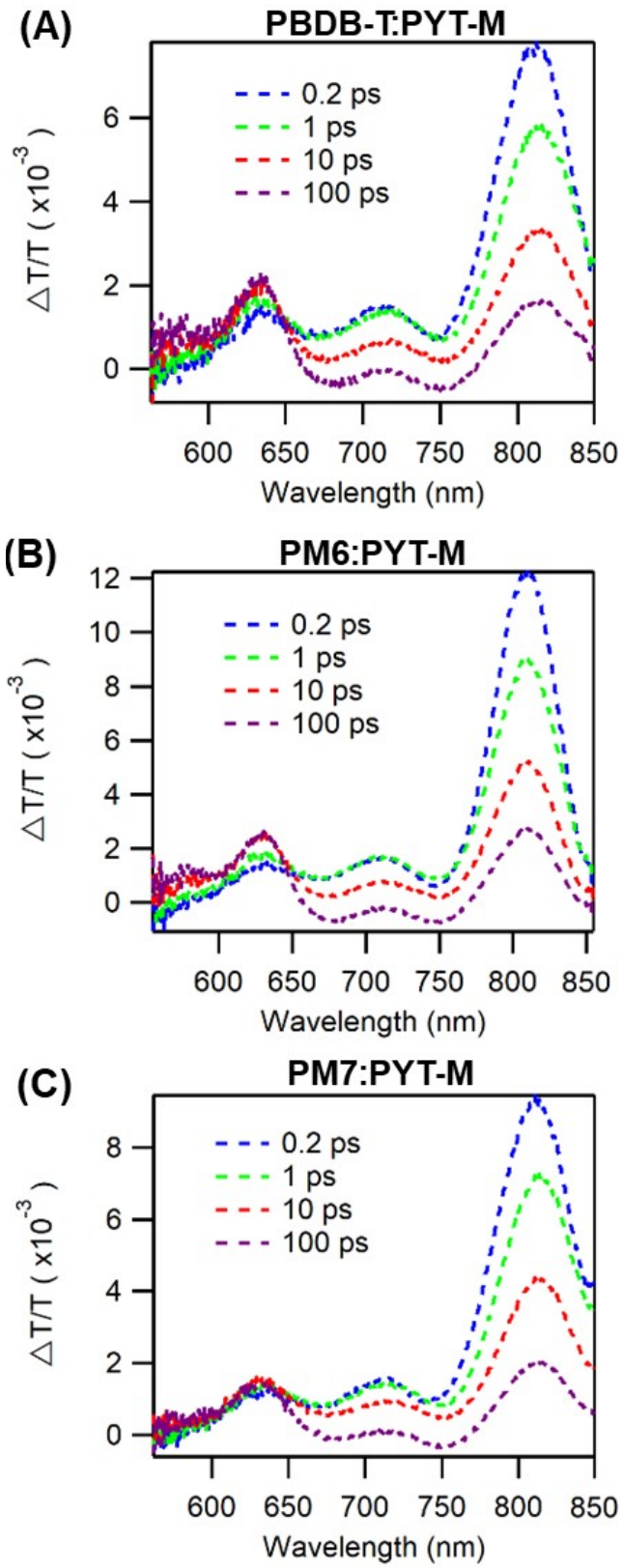

Figure S10. TA spectra of (A) the PBDB-T:PYT-M film, (B) the PM6:PYT-M film and (C) PM7:PYT-M film at indicated delay times.

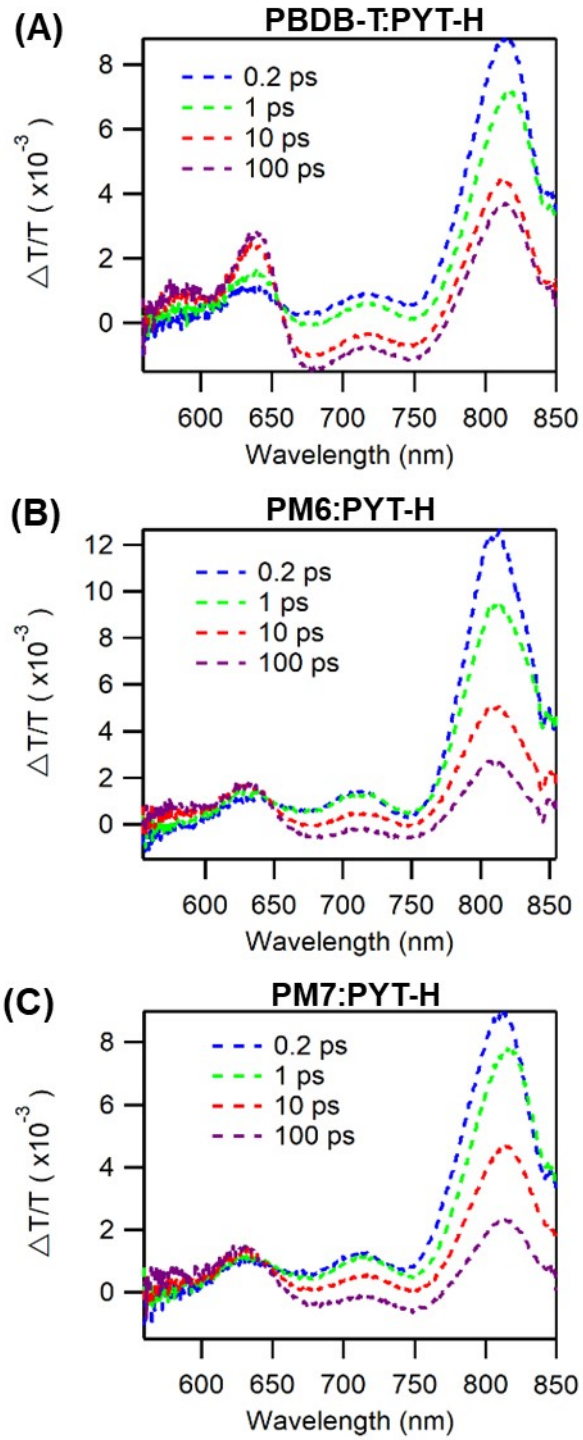

Figure S11. TA spectra of (A) the PBDB-T:PYT-H film, (B) the PM6:PYT-H film and (C) PM7:PYT-H film at indicated delay times.

Table S4. The kinetics parameters of the HT processes of the corresponding films, calculated from femtosecond transient absorption spectroscopy.

Sample		A_1	τ_1 (ps)	A_2	τ_2 (ps)
PYT-M	PBDB-T	60.2%	0.107±0.011	39.8%	9.32±0.93
	PM6	58.2%	0.194±0.019	41.8%	8.79±0.80
	PM7	76.9%	0.110±0.011	23.1%	11.37±1.14

	PBDB-T	57.5%	0.182±0.018	42.5%	8.69±0.87
PYT-H	PM6	49.5%	0.211±0.021	50.5%	9.28±0.93
	PM7	65.4%	0.112±0.011	34.6%	10.08±1.01

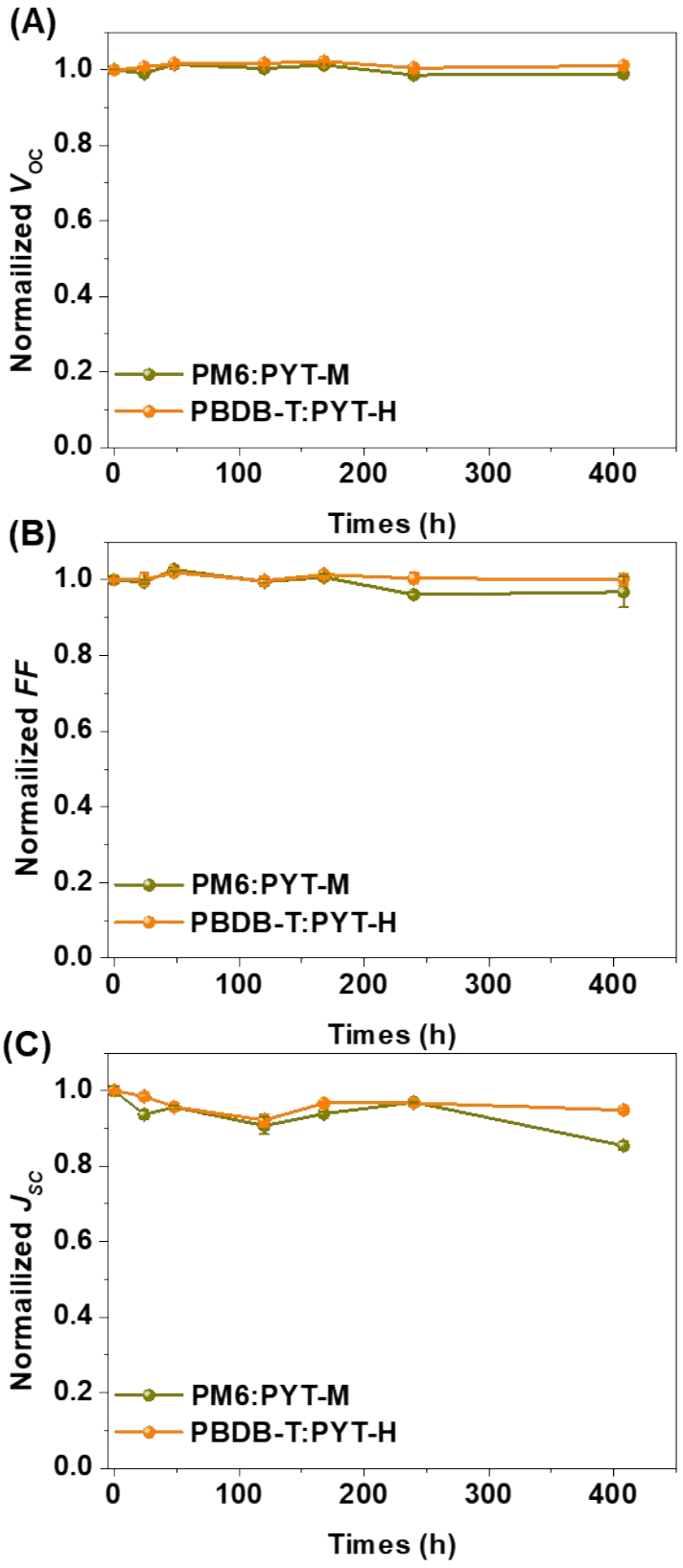

Figure S12. Changes of (A) normalized V_{OC}, (B) FF, (C) normalized J_{SC} losses based on PM6:PYT-M and PBDB-T:PYT-H solar cells with each system for four cells, annealed at 85 °C at room temperature in the nitrogen glovebox.

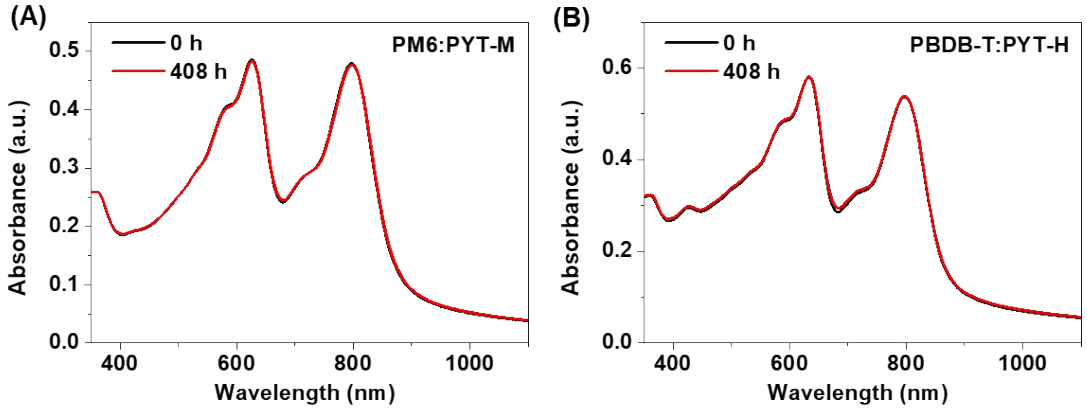

Figure S13. Variation of UV-absorption spectra of the devices based on PM6:PYT-M and PBDB-T:PYT-H, annealed at 85 °C at room temperature in the nitrogen glovebox.

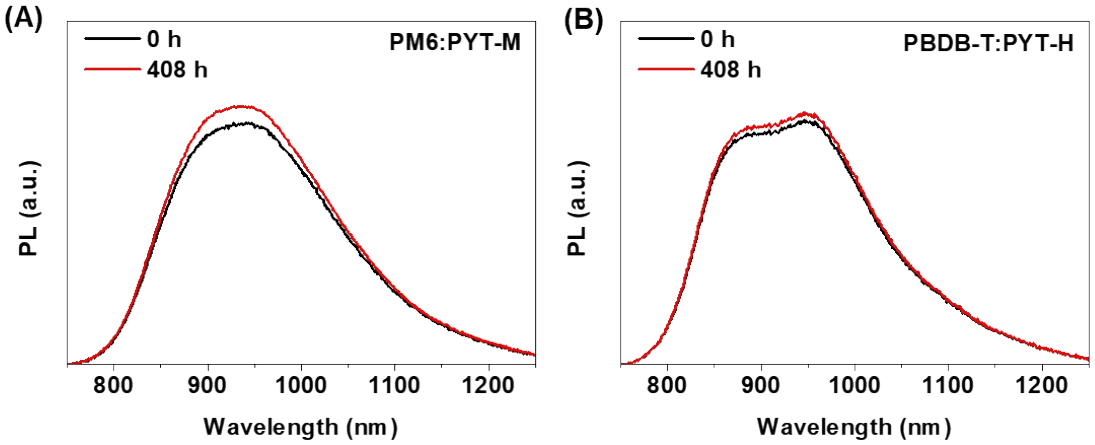

Figure S14. Variation of PL spectra of the devices based on PM6:PYT-M and PBDB-T:PYT-H, annealed at 85 °C at room temperature in the nitrogen glovebox.

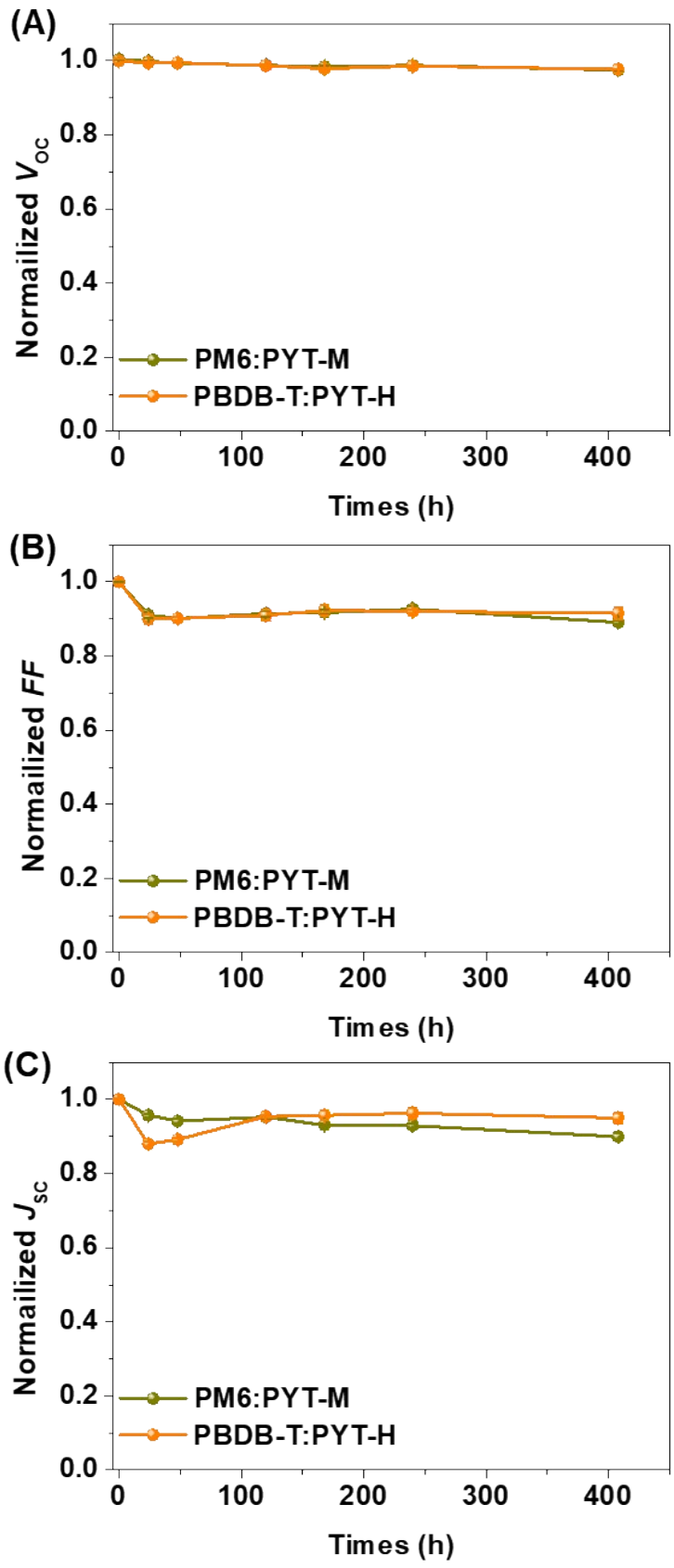

Figure S15. Changes of (A) normalized V_{OC}, (B) FF, (C) normalized J_{SC} losses over illumination time for PM6:PYT-M and PBDB-T:PYT-H solar cells with each system for four cells.

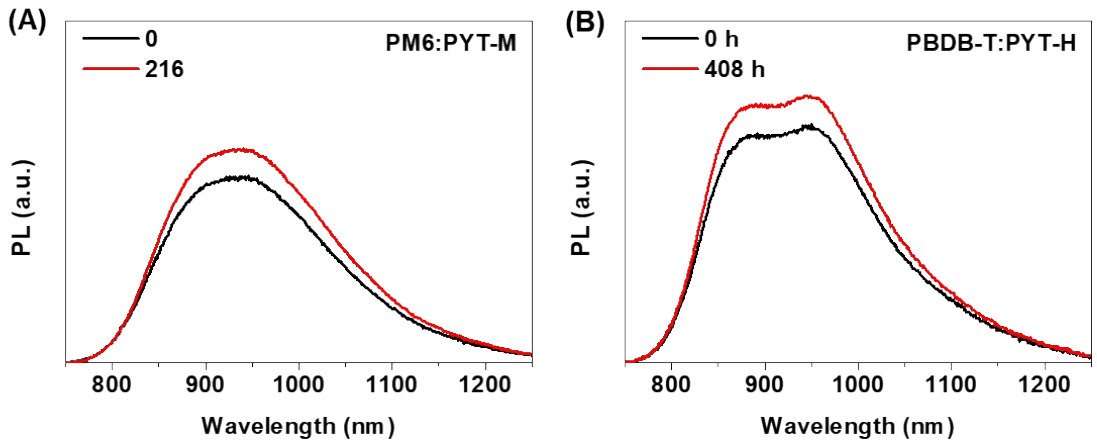

Figure S16. Variation of PL spectra of the devices based on PM6:PYT-M and PBDB-T:PYT-H, annealed at 85 °C at room temperature in the nitrogen glovebox.

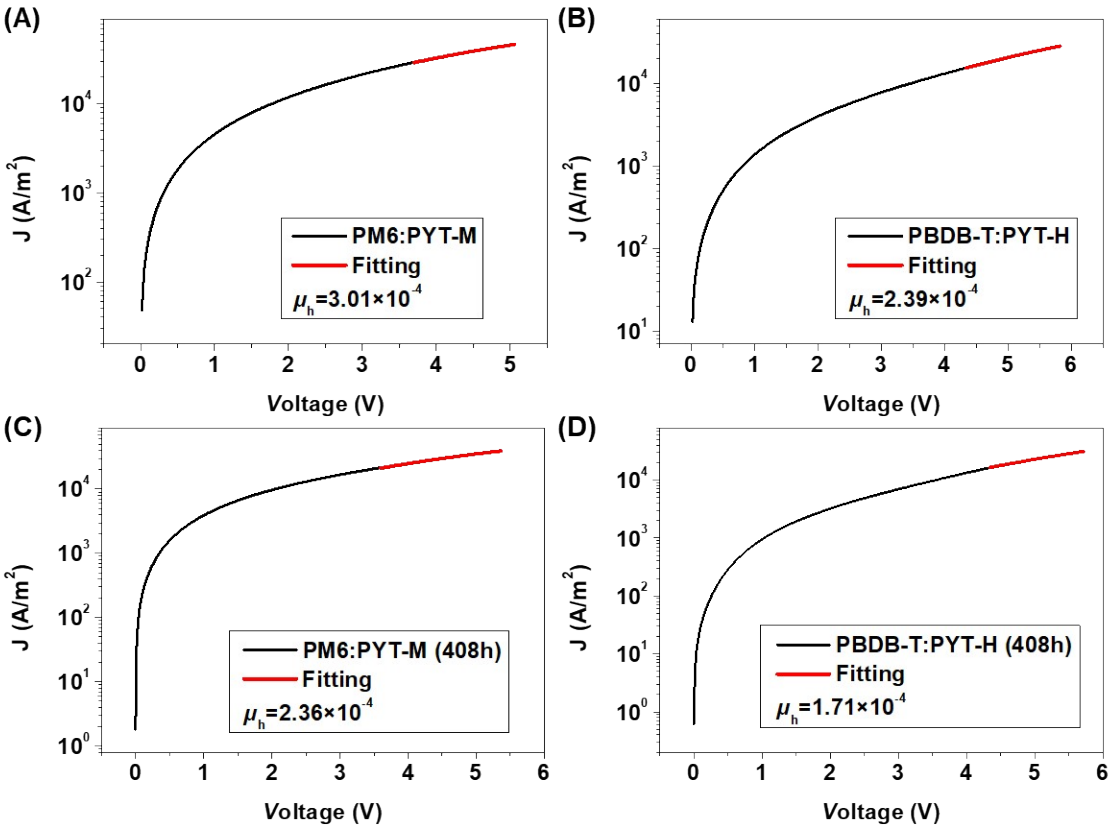

Figure S17. The dark *J-V* characteristics of hole-only mobility of (A) PM6:PYT-M and (B) PBDB-T:PY-S blend films for 0 hours. The dark *J-V* characteristics of hole-only mobility of (C) PM6:PYT-M and (D) PBDB-T:PYT-H blend films under one sun illumination for 408 hours. The red lines represent the best fitting using the SCLC model. The inset mobility data are average values of four diodes.

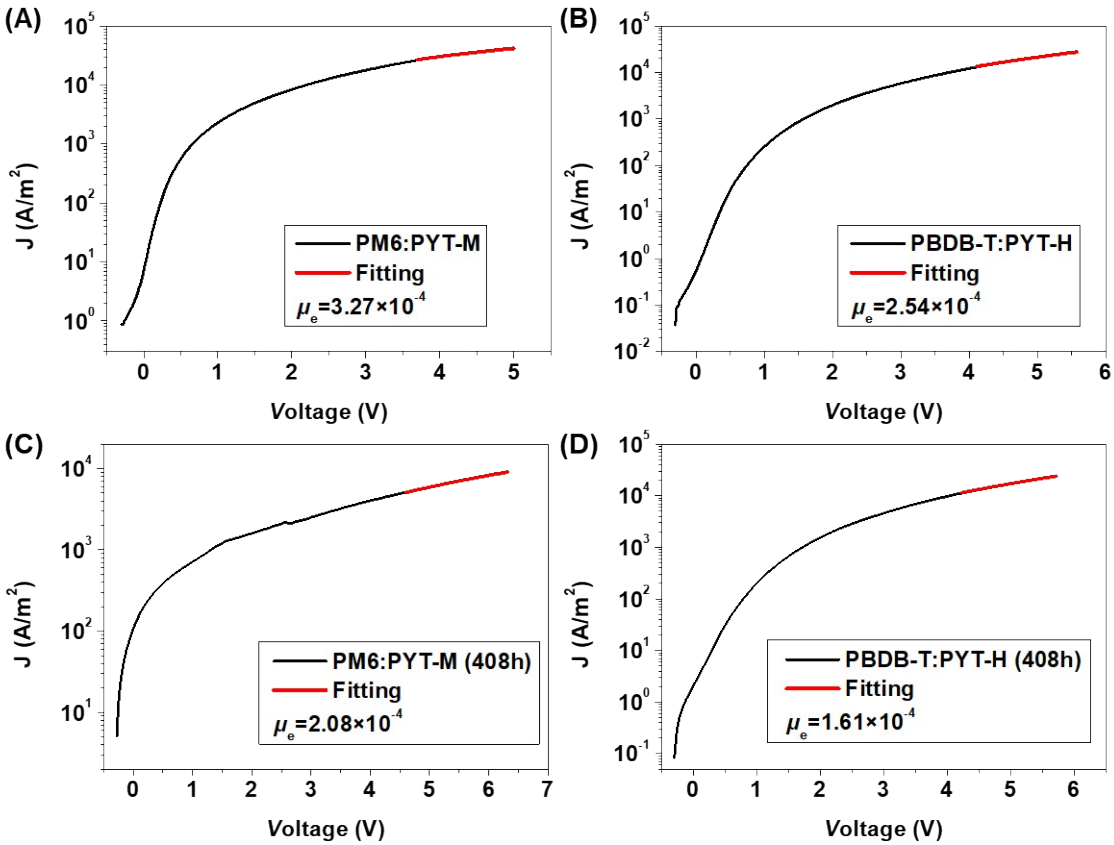

Figure S18. The dark *J-V* characteristics of electron-only mobility of (A) PM6:PYT-M and (B) PBDB-T:PYT-H blend films for 0 hours. The dark *J-V* characteristics of hole-only mobility of (C) PM6:PYT-M and (D) PBDB-T:PY-S blend films under one sun illumination for 408 hours. The red lines represent the best fitting using the SCLC model. The inset mobility data are average values of four diodes.

Table S5. The properties of PM6:PYT-M and PBDB-T:PYT-H devices under light soaking.

Sample	Time (Light stability)	Increased quenching efficiency	μ_e ($\times 10^4$ cm^{-1})	μ_h ($\times 10^4$ cm^{-1})	μ_e/μ_h	R[a]
PM6:PYT-M	0 h	14.35%	3.27	3.01	1.09	2.06
	408 h		2.08	2.36	0.88	2.18
PBDB-T:PYT-H	0 h	12.58%	2.54	2.39	1.06	2.02
	408 h		1.61	1.71	0.94	2.11

[a]The carrier recombination order calculated from the TPV and CE measurements.

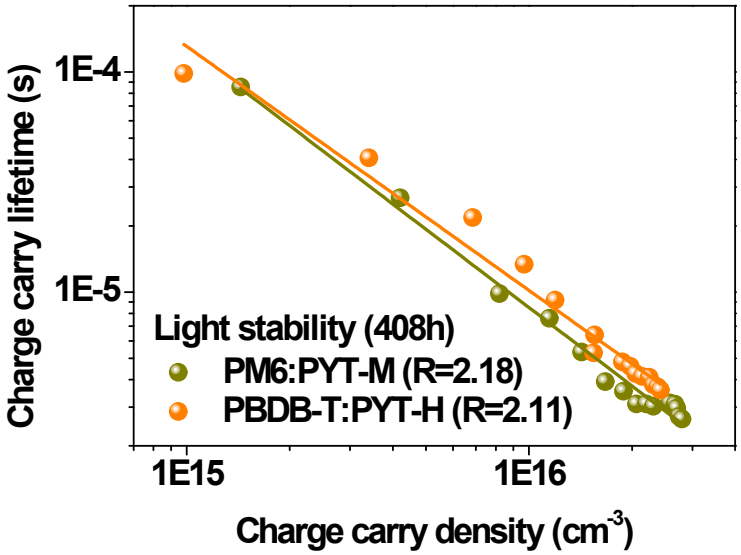

Figure S19. Charge carrier lifetime τ, obtained from TPV, as a function of charge density n, calculated from CE under V_{OC} conditions (from 0.15 to 2.50 suns). The devices were exposed after 408 hours under one sun illumination in N_2-filled glovebox.

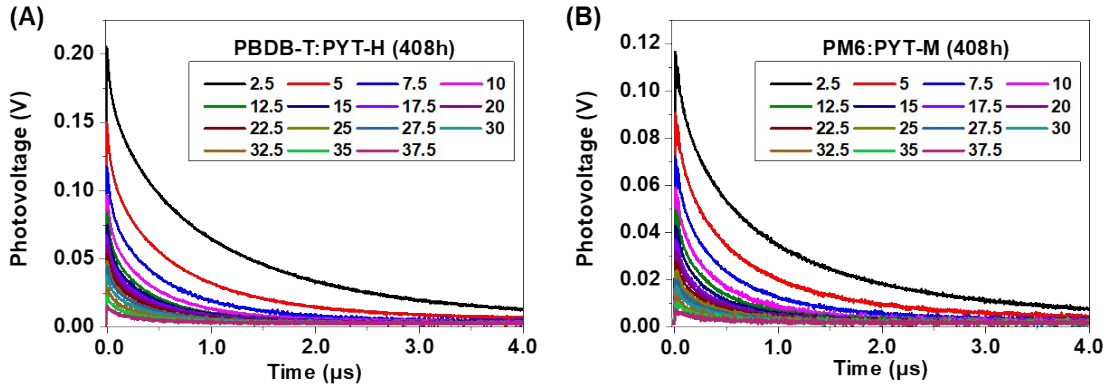

Figure S20. TPV measurements on the light-soaking devices (408h) of (a) PBDB-T: PYT-H, (b) and PM6:PYT-M devices for light intensities of 0.15 to 2.50 sun.

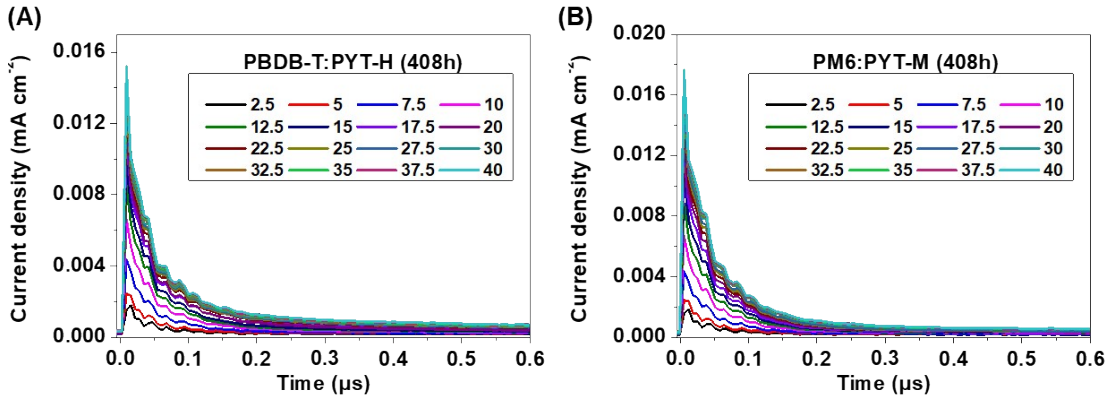

Figure S21. CE measurements on the light-soaking devices (408h) of (a) PBDB-T: PYT-H, (b) and PM6:PYT-M devices for light intensities of 0.15 to 2.50 sun.

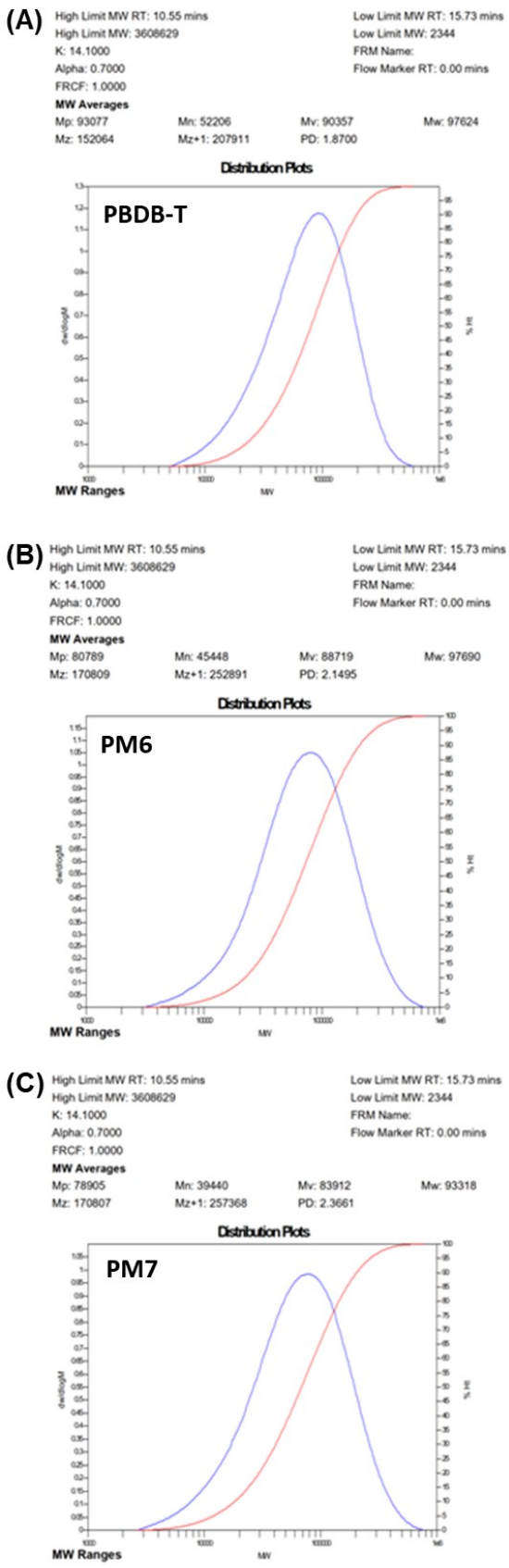

Figure S22. Distribution plots of gel permeation chromatography (GPC) measured at 150 °C using 1, 2, 4-trichlorobenzene as the eluent. Molecular weight for PBDB-T, PM6 and PM7**.**

Reference:

1. W. Wang, Q. Wu, R. Sun, J. Guo, Y. Wu, M. M. Shi, W. Y. Yang, H. N. Li, J. Min, Joule 2020, 4, 1070-1086.
2. Q. Wu, W. Wang, T. Wang, R. Sun, J. Guo, Y. Wu, X. C. Jiao, C. J. Brabec, Y. F. Li, J. Min, Sci. China Chem. 2020, 63, 1449-1460.
3. Q. Wu, W. Wang, Y. Wu, Z. Chen, J. Guo, R. Sun, J. Guo, Y. Yang, J. Min, Adv. Funct. Mater. 2021, 2010411.
4. Z. Zheng, H. Yao, L. Ye, Y. Xu, S. Zhang, J. Hou, Mater. Today 2019, 35, 115-130.
5. S. Zhang, Y. Qin, J. Zhu, J. Hou, Adv. Mater. 2018, 30, 1800868.